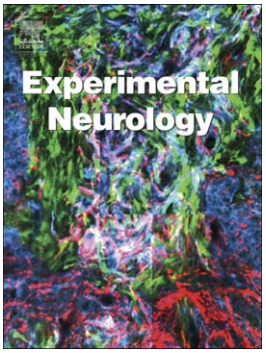

A neural cell adhesion molecule-derived peptide, FGL, attenuates glial cell activation in the aged hippocampus

Bunmi Ojo, Payam Rezaie, Paul L. Gabbott, Thelma R. Cowely, Nikolay I. Medvedev, Marina A. Lynch, Michael G. Stewart

PII: S0014-4886(11)00333-5
DOI: doi: 10.1016/j.expneurol.2011.09.025
Reference: YEXNR 10915

To appear in: *Experimental Neurology*

Received date: 17 May 2011
Revised date: 10 August 2011
Accepted date: 15 September 2011

Please cite this article as: Ojo, Bunmi, Rezaie, Payam, Gabbott, Paul L., Cowely, Thelma R., Medvedev, Nikolay I., Lynch, Marina A., Stewart, Michael G., A neural cell adhesion molecule-derived peptide, FGL, attenuates glial cell activation in the aged hippocampus, *Experimental Neurology* (2011), doi: 10.1016/j.expneurol.2011.09.025

A neural cell adhesion molecule-derived peptide, FGL, attenuates glial cell activation in the aged hippocampus

Bunmi Ojo[1], Payam Rezaie[1], Paul L. Gabbott[1], Thelma R. Cowely[2], Nikolay I. Medvedev[1], Marina A. Lynch[2], and Michael G. Stewart[1]*

[1]Department of Life Sciences, The Open University, Walton Hall, Milton Keynes MK7 6AA, UK; [2]Trinity College Institute of Neuroscience, Trinity College, Dublin 2, Ireland.

Running Title: FGL attenuates age-related glial activation

***Correspondence to:**

Michael G. Stewart PhD
Professor of Neuroscience
Department of Life Sciences
Faculty of Science
The Open University
Walton Hall
Milton Keynes
MK7 6AA
United Kingdom
Tel: +44(0)1908653448
Fax: +44(0)190865416
E-mail: m.g.stewart@open.ac.uk

Abstract

Neuroglial activation is a typical hallmark of ageing within the hippocampus, and correlates with age-related cognitive deficits. We have used quantitative immunohistochemistry and morphometric analyses to investigate whether systemic treatment with the Neural Cell Adhesion Molecule (NCAM)-derived peptide FG Loop (FGL) specifically alters neuroglial activation and population densities within the aged rat hippocampus (22 months of age). A series of 50µm paraformaldehyde/acrolein-fixed sections taken throughout the dorsal hippocampus (5 animals per group) were immunostained to detect astrocytes (GFAP and S100ß) and microglial cells (CD11b/OX42 and MHCII/OX6), and analyzed using computerised image analysis and optical segmentation (Image-Pro Plus, Media Cybernetics). FGL treatment reduced the density of CD11b+ and MHCII+ microglia in aged animals, concomitant with a reduction in immunoreactivity for these phenotypic markers. FGL treatment also markedly reduced GFAP immunoreactivity within all hippocampal subfields in aged animals, without exerting an appreciable effect on the density of S100ß+ cells. These results demonstrate that FGL can indeed regulate neuroglial activation and reduce microglial cell density in the aged hippocampus, and support its potential use as a therapeutic agent in age-related brain disorders.

Keywords: Ageing, Microglia, Astrocytes, Hippocampus, NCAM-derived peptide

Introduction

Ageing is associated with impairments in hippocampal function (Barnes, 1988; Murray and Lynch 1998), an altered neuroinflammatory response (Conde and Streit, 2006; David et al., 1997; Sheng et al., 1998), and an increased likelihood of developing neurodegenerative diseases.

The underlying neuroinflammatory response, typified by neuroglial (astrocyte and microglial) activation and increased pro-inflammatory cytokine production, has been correlated to a deficit in synaptic plasticity and impairment in hippocampal-dependent tasks. (Clarke et al., 2008; Frautschy et al., 2001; Griffin et al., 2006; Lynch and Lynch, 2002; Lynch, 2004; 2009). Reducing neuroinflammation within the brain of aged animals rescues some of these deficits. For example, inhibiting either glial cell activation (Griffin et al., 2006) or limiting the concentration of the major pro-inflammatory cytokine IL-1ß (Frautschy et al., 2001; Lynch et al., 2007) attenuates age-associated deficits in cognitive function. Pharmacological interventions targeting neuroinflammation would therefore be expected to minimise the heightened vulnerability of the brain in ageing.

Previous work from our group has shown that the NCAM-derived peptide, FGL, can act as a novel anti-inflammatory agent in models of ageing and age-related diseases, restoring cognitive function and averting neuropathology (Downer et al., 2010; Cambon et al., 2004; Klementiev et al., 2007; Neiiendam et al., 2004; Popov et al., 2008; Skibo et al., 2005; Stewart et al., 2010). NCAM plays an important role in the nervous system in development, plasticity and learning and memory (Berezin et al., 2000; Cavallaro et al., 2002; Cremer et al., 1994; Crossin and Krushel, 2000; Luthl et al., 1994). The NCAM signalling transduction cascade is initiated by direct interaction of NCAM with fibroblast growth factor receptor (FGFR), expressed on both neurons and glial cells (Berezin and Bock, 2004; Kiselyov et al., 2003; Walmond et al., 2004). FGL is a 15 amino acid peptide synthesised from the interconnecting loop region of the second fibronectin type III module in the extracellular domain of NCAM, which interacts with the binding site of FGFR1 (Berezin and Bock 2010; Hansen et al. 2010; Kiselyov et al., 2003; Walmond et al., 2004). FGL has been shown to activate FGFR1 on neurons and glia, mimicking the heterophilic interaction between NCAM and FGFR1 (Walmond et al., 2004).

The aim of the present study was to investigate whether systemic treatment with FGL *in vivo* alters astrocyte and microglial activation states and population densities within the aged rat hippocampus. Our results show that FGL treatment significantly reduced the density of MHCII/OX6+ and CD11b/OX42+ microglia as well as immunoreactivity for these cellular

markers within the hippocampus of aged animals. FGL treatment also markedly reduced astrocytic GFAP immunoreactivity within all hippocampal subfields in aged animals, but did not appreciably affect astrocytic S100ß+ cell density estimates. Neuroglial activation is believed to contribute towards age-related cognitive dysfunction. Our results provide persuasive evidence that FGL can attenuate glial cell activation and reduce microglial cell density in the aged brain. The potential for FGL to improve or to prevent age-related cognitive decline therefore warrants further investigation.

Materials and Methods

Animals

Male Wistar rats aged 4 months (250-350g) or 22 months (450–550 g) supplied from Harlan UK, were reared under specific pathogen-free conditions until they arrived in Trinity College Dublin, where they were housed in pairs under a 12-h light schedule at ambient temperature controlled between 22°C and 23°C. Animals were maintained under veterinary supervision throughout the study. There was no evidence of any disease, including any former history of infection, amongst the colony investigated. Healthy (young and aged rats) were used in this study. Experiments were performed under a license issued by the Department of Health (Ireland) and in accordance with the guidelines approved by the local ethical committee at Trinity College Dublin.

Treatment

Animals were injected subcutaneously with 8 mg/kg FGL_L (5 mg/ml solution in sterile water) or with the same volume of vehicle (sterile water), on alternate days, receiving 10 doses in total, the first on experimental Day 1 and the last on Day 19. The FGL peptide was sourced from Polypeptide Laboratories (Hillerod, Denmark) (Klementiev et al., 2007). Purity was estimated by HPLC and MALDI-TOF MS (VG TOF Spec E, Fisons Instruments, Beverly, MA, USA). The injected form of the peptide is dimeric and consists of two FGL monomers linked at the N-terminal. This dimeric form was previously selected for clinical development (Anand et al., 2007). The dose and route of administration was based on previous publications (Downer et al., 2010; Secher et al., 2006). Previous studies, using the same treatment regime described here, demonstrated that FGL crossed the blood–brain barrier within 10 min of injection and remained detectable in the cerebrospinal fluid (CSF) for up to 5 hours (see for example, Secher et al., 2006). Blood plasma levels of FGL were up to 10-fold higher than in CSF during the first 2 hours after administration (Secher et al., 2006). On Day 20 rats were prepared for light microscopic examination.

Tissue preparation and processing for light microscopy

Animals were deeply anesthetised with urethane (1.5 g/kg), perfused transcardially with 100mL of physiological saline, followed by 100 mL of 3.5% paraformaldehyde and 3.75% acrolein in 0.1M phosphate buffer (pH 7.4) at room temperature. After perfusion, the brains were removed from the skull, post-fixed and placed in 0.1M phosphate buffer solution. Forebrain blocks, which included the dorsal anterior hippocampus, were marked to allow subsequent identification. A consecutive series of 50µm-thick coronal sections, cut using a vibratome from the right dorsal anterior hippocampus (bregma co-ordinates -1.80mm to 4.16mm; Paxinos and Watson, 2007), were collected for light microscopic examination. Five separate series of sections (taking every sixth section, averaging around ten sections per series) were selected for each animal; one series for volume estimation, and the other four series for immunohistochemical staining.

Light-microscopy: volume estimation

The volume of the right dorsal anterior hippocampus in control and FGL treated animals was determined by quantitative light microscopy using the Cavalieri method (Pakkenberg and Gundersen, 1997) as described elsewhere in relation to hippocampus (Popov et al., 2004; Stewart et al., 2005). In brief, rostrocaudal sections from right dorsal anterior hippocampus of each animal (taking every sixth serial section) were mounted onto glass slides and stained with a solution of 0.1% Toluidine Blue in 0.1 M PB (pH 7.4) for 2 min. Stained sections were viewed at low magnification using a Nikon E600 digital photomicroscope. Digital images were captured electronically and displayed on a computer screen. For each animal (n=5-6 per group), the total volume of the right dorsal anterior hippocampus was subsequently derived by multiplying the calculated mean surface area by the section thickness (t=50 µm) and the total actual number of sections (n) in which the right dorsal anterior hippocampus occurred.

Immunohistochemical staining of rat brain sections

Four separate series of 50 µm-thick sections taken throughout the extent of the right dorsal anterior hippocampus (averaging ten sections per animal, n=5 animals per group) were immunostained in entire batches with antibodies raised against GFAP (rabbit anti-GFAP, 1:1000, Dako), and S100ß (rabbit anti-S100ß , 1:8000, Dako) to detect astrocytes, and with antibodies raised against CD11b (mouse anti-rat CD11b, clone OX42, 1:400, Abcam) and Major Histocompatibility Complex Class II (mouse anti-rat MHCII, clone OX6, 1:100, Abcam) for microglia. Sections were rinsed overnight at room temperature in a solution of phosphate buffer (PB: 0.1M, pH 7.4) and treated for 30 minutes with [0.26M] sodium borohydride ($NaBH_4$). After rinsing, sections were immersed for 1 hour in endogenous peroxidase blocking solution (10% methanol in deionised water, to which 3% hydrogen peroxide solution was

added). Sections were then incubated with 10% normal horse serum (for OX-42 and OX-6) or swine serum (for GFAP and S100ß) containing 0.01% Tween 20, for a period of 2 hours and then transferred to primary antibody solution made up in 1% normal horse/swine serum with 0.01% Tween 20, and incubated overnight on a shaker at room temperature. Sections were rinsed three times with PB and transferred to a solution containing secondary antibody (for microglial markers OX-42 and OX-6: biotinylated horse anti-mouse 1:100, Abcam; for astrocyte markers GFAP and S100ß: biotinylated swine anti-rabbit 1:200, Dako) for 2 hours. Sections were rinsed three times with PB and incubated for 1 hour with avidin-biotin-horseradish peroxidase solution (Vectastain Elite ABC kit; Vector Laboratories) in PB containing 0.01% Tween 20. After washing, immunoreactivity was visualised with 3,3.-diaminobenzidine (DAB) chromogen, and 0.05% hydrogen peroxide. Sections were processed in entire batches for each antibody (cell marker). Development with the chromogen was timed and applied as a constant across batches to limit technical variability (in immunodetection) before progressing to quantitative image analysis (see Brey 2003). The reaction was terminated by rinsing sections in distilled water. Finally, sections were mounted onto gelatin-coated glass slides, progressed through a graded series of alcohols (dehydrated), cleared in xylene and coverslipped with PerTex mounting medium. Negative control sections were included where the primary antibody was omitted and replaced either with blocking serum (10% normal horse or swine serum) or biotinylated secondary antibodies alone (horse anti-mouse or swine anti-rabbit). Immunoreacted sections were viewed with a Nikon light microscope.

Image analysis and cell density measurements

Immunoreactivity for glial cell markers GFAP, CD11b (OX42) and MHC-II (OX6) was measured by quantitative image analysis (optical segmentation) using Image-Pro Plus software (Media Cybernetics, Europe), as previously described (Leuba et al. 1998; Milnerwood et al. 2006; Pontikis et al. 2004; Rezaie et al. 2005), with each marker analyzed blind with respect to grouping. Immunoreactivity for each cell marker was assessed within the corpus callosum (which served as an internal reference) and within the dentate gyrus/hilus, CA3 and CA1 subfields of the hippocampus (spanning the stratum pyramidale, and partially the stratum oriens and stratum radiatum on either side) (Paxinos and Watson 2007). A survey of immunoreacted tissue sections was performed independently to verify specific immunoreactivity in each series of sections subsequently progressed to quantitative image analysis. Briefly, non-overlapping RGB images were digitally captured at random within the defined areas from each section in the series, providing a systematic survey of each region throughout the dorsal hippocampus for each animal within a group. Images were captured via a digital camera (JVC KY-F75V) mounted onto a Nikon Microphot-FX microscope (Nikon UK Ltd) using a x20 objective and neutralizing grey filters. All parameters including the lamp intensity, digital camera setup, microscope and

video calibration were held constant. A minimum of 30 microscopic fields were analysed per region, per animal. Individual microscopic fields measured 295µm x 220µm, giving a total area of 1.947mm^2 examined for each hippocampal subfield per animal (n=5 animals per group). Optical segmentation of immunoreacted profiles was analysed using Image-Pro Plus morphometric image analysis software (version 5.0, Media Cybernetics) as previously described (Milnerwood et al. 2006; Pontikis et al. 2004; Rezaie et al. 2005).

Quantitative immunohistochemistry, using computerised image analysis and optical segmentation techniques (or densitometric analysis), is an established procedure used in modern clinical and experimental histopathology (Brey et al., 2003; Campuzano et al., 2008; Cotter et al., 1997; Kokolakis et al., 2008; Peretti-Renucci et al., 1991; Wang et al., 2009; Zehntner et al., 2008), with strong test-retest reliability, that allows comparative analysis of immunostained sections (captured as images) to be made in different laboratories (Brey et al., 2003; Dobson et al., 2010). Commercially available image analysis programmes, such as used here (see Xavier et al. 2005), are an aid to standardise interpretation. A correlation between immunohistochemical staining and protein levels has also been shown independently using Western blot and immunoassays (see Brey 2003). There are a number of ways to measure the 'level' of immunohistochemical stain (Brey et al., 2003; Mize et al., 1988). In this study we examined the area of tissue stained with DAB (percent area), defined as the area of the image classified as stained with DAB, divided by the total image area. Given that nuclear stains often confound the results of imaging techniques, the 'pure' DAB stain was analysed giving optimal results. We applied rigorous staining protocols, outlined above, to ensure consistency of immunostaining, and accuracy of image analysis. The procedure has been previously described (Milnerwood et al. 2006; Pontikis et al. 2004; Rezaie et al. 2005). A semi-automated RGB histogram-based protocol (specified in the image analysis programme) was employed to determine the optimal segmentation (threshold setting) for immunoreactivity for each antibody.

Briefly, each RGB image was processed using a constant 'colour-cube' segmentation setting, with a threshold selected that most accurately defined foreground immunostaining for each antibody (corresponding to the averaging of the highest and lowest immunoreactivities within the sample population), and this optimal segmentation (threshold setting) was then applied as a constant to all subsequent images analyzed for this antibody. Furthermore, the specificity of the detection method was also verified manually by monitoring the analysis as it progressed, per region, per animal. Immunoreactive profiles were discriminated in this manner to determine the specific immunoreactive area (the mean RGB value obtained by subtracting the total mean RGB value from non-immunoreacted value per defined field). Macros were subsequently recorded to transfer the data to a spreadsheet for subsequent statistical analysis. Data were separately plotted

as the mean percentage area of immunoreactivity per field (denoted "% Area") ± standard error of the mean (SEM) for each region and grouping.

Areal cell density values (number of cells/mm²) (see also Dalmau et al., 2003; Savchenko et al., 2000) were calculated for S100ß+, CD11b(OX42)+ and MHCII(OX6)+ glial cells within each of the hippocampal subfields, based on cell counts made in the same 1-in-5 series of immunoreacted tissues sections that underwent quantitative image analysis described above. The analysis was carried out in a systematic manner; for each cell marker, a minimum of 30 non-overlapping RGB images (microscopic fields using a x40 objective) were captured randomly within each hippocampal subfield across an average of ten sections per animal, giving a minimum area of 0.504mm^2 analysed per subfield, per animal (n=5 animals per group). S100ß+, CD11b, MHCII cell somata and processes could be reliably discriminated in these images. To obtain cell density estimates, only cell somata identified within the confines of each image were manually counted. Partially intersected cell somata were not counted if present (e.g. located at edges of each image). For each hippocampal subfield, cell density values were determined by dividing the total cell number across all images by the total area analysed in mm^2 (see Dalmau et al., 2003; Savchenko et al., 2000). Cell counts within tissue sections immunoreacted with GFAP could not be reliably determined owing to section thickness resulting in a dense pattern of labelling of astrocyte processes, particularly in aged animals that obscured cell somata. In contrast, astrocytic cell somata were prominently labelled with S100ß, and these sections were therefore progressed to cell density measurements as described. Data were plotted as total cell counts per unit area examined (number of cells/mm^2) ± SEM.

mRNA expression analysis (GFAP, S100ß)

RNA was extracted from hippocampal tissue (4 month and 22 month old animals treated with vehicle or FGL, n=5-6) using a NucleoSpin RNAII isolation kit (Macherey-Nagel Inc., Germany) according to the manufacturer.s instructions. RNA concentrations were equalized to 1µg prior to cDNA synthesis using a High Capacity cDNA RT Kit (Applied Biosystems, UK) according to the manufacturer's instructions. Equal concentrations of cDNA were used for RT-PCR amplification. Real-time PCR primers were delivered as "Taqman® Gene Expression Assays" containing forward and reverse primers, and a FAM-labelled MGB Taqman probe for each gene (Applied Biosystems, UK) as described previously (Downer et al., 2009). The assay IDs for the genes examined were as follows: GFAP (Rn00566603_m1), S100ß (Rn00566139_m1). Gene expression was calculated relative to the endogenous control samples (ß-actin; #4352340E, Applied Biosystems, Foster City, CA) to give a relative quantification (RQ) value (2^{-DDCT}, where CT is threshold cycle).

Statistical analysis

Graphs were prepared using Prism 5.0 software, and data analysed using the Statistical Package for the Social Sciences program (SPSS version 17, SPSS Inc., Chicago, USA). One- way analysis of variance (ANOVA) was used with criterion $p<0.05$ to assess group differences, followed by Tukey.s unequal N honest significant differences test (for immunoreactivity, volume and cell density estimates). Two-way ANOVA was used with criterion $p<0.05$, applying Bonferroni's post hoc test to assess differences between groups for mRNA expression levels.

Results

Hippocampal volume

The mean total (right) dorsal hippocampal volume in aged vehicle-treated rats was 9.69 ± 0.47 mm^3 (mean ±s.e.m, n=5) and in FGL treated aged rats, it was 9.89 ± 0.65 mm^3 (mean ± s.e.m, n=6), showing no significant differences between treatments (p=0.807). In young vehicle-treated rats the total (right) dorsal hippocampal volume was 11.30 ± 0.47mm^3 (mean ± s.e.m, n=5), and for young FGL-treated rats the right dorsal hippocampal volume was 8.56 ± 0.41 mm^3 (mean ± s.e.m, n=6). Because this difference was significant (p>0.05), the cell density values for young FGL-treated rats shown in Figure 4 (see Fig. 4B, 4D, 4F), should be interpreted with caution (since treatment-related volume changes could contribute to density differences). However, there were no hippocampal volume differences associated with treatment in aged rats, and cell density data for aged (FGL and vehicle-treated) animals are presented in Figure 5 (see Fig. 5B, 5D and 5F).

Morphologic and phenotypic changes in astrocytes and microglia with age

Figures 1 and 2 show age-related changes in morphology and phenotype of GFAP+ (Fig. 1A-H, Q,R) and S100β+ (Fig. 1I-P,S,T) astrocytes, CD11b+ (Fig 2. A-H,Q,R) and MHCII+ (Fig2. I-P,S,T) microglia within the corpus callosum and hippocampus of rats treated with vehicle alone. The pattern of staining of glial cell markers was considerably less intense in younger animals for GFAP, CD11b and MHCII (e.g. for GFAP, compare Fig. 1A,C,E,G,Q (4months) with B,D,F,H,R (22 months); for CD11b compare Fig. 2A,C,E,G,Q (4months) with B,D,F,H,R (22 months); and for MHCII compare Fig. 2I,K,M,O,S (4 months) with J,L,N,P,T (22 months). Upregulation of the intermediate filament GFAP in astrocytes, is typically associated with an increase in the activation state of these cells (Amenta et al., 1998; Geinisman et al., 1978; Hughes and Lantos, 1987). In aged animals, GFAP+ astrocytes exhibited thicker processes, and hypertrophic cell somata while maintaining their stellate morphology. These cells were widely and uniformly distributed throughout the hippocampus in aged animals (Fig. 1R).

S100ß is a calcium-binding protein, known to be expressed by all types of astrocytes; it prominently labels astrocyte cell somata within the CNS (Rothermundt et al., 2003; Sen and Belli, 2007, Savchenko et al., 2002). We have used S100ß labelling because it specifically identifies 'all populations' of astrocytes (including fibrous and protoplasmic, resident as well as activated), allowing us to reliably look at 'total' astrocyte population dynamics. S100ß is known to be expressed by GFAP+ cells (Rothermundt et al., 2003; Sen and Belli, 2007). Levels of both markers have been shown to increase following activation of astrocytes (Himeda et al., 2006; Pelinka et al., 2004; Yasuda, 2004), although differences have also been noted in expression dynamics/profiles (Savchenko et al., 2002; Yasuda et al., 2004). We found no appreciable change in S100ß immunoreactivity within the hippocampus in aged (compared to young) animals, see Fig. 1I,K,M,O,S (4 months) with 1J,L,N,P,T (22 months).

De novo expression or upregulation of MHC class II molecules on microglia is taken as a specific indicator of the immune 'activation state'/antigen-presenting capability of microglial cells (Ogura et al., 1994; Rozovsky et al., 1998). CD11b (present on both activated and non-activated resident microglia – Lawson et al., 1990; Ogura et al., 1994) was used to further specify alterations in microglia activation status. In our samples, the CD11b antibody consistently labelled process-bearing perivascular and parenchymal microglia cells within the dorsal anterior hippocampus and overlying corpus callosum (Fig. 2A-H,Q,R). We did not see any evidence of infiltrating cells (monocytes, macrophages, granulocytes or natural killer cells) within the areas investigated in any of the animals including aged animals. As expected, relatively little MHCII staining was observed within the hippocampus of younger animals (Fig. 2I,K,M,O,S), the most intense staining being confined to the corpus callosum (Fig. 2I). The pattern of staining in aged animals was much more intense and widespread, with a clear increase in MHCII+ staining within the corpus callosum (Fig. 2J), CA3 (Fig. 2N) and DG/hilus (Fig. 2P), but little reactivity within the CA1 subfield (Fig. 2L,T). Remarkably few MHCII+ cells were found within the CA1 subfield of the hippocampus at both ages (Fig. 2S,T). By comparison, CD11b staining was more intense and widespread within the hippocampus (see Fig. 2R) at 22 months of age, including within the CA1 (Fig. 2D), as well as the CA3 (Fig. 2F) of aged animals. Comparative differences in immunolabelling with MHCII and CD11b could either reflect changes in population densities of microglia, or dynamic changes in expression of these cellular markers by a stable population of resident cells (i.e. a change in the functional activation state of microglia, regionally). In aged animals, MHCII+ and CD11b+ microglia displayed more prominent cell bodies, with thickened processes, frequently adopting a more 'bushy' ramified morphology (see Fig. 2F,J,N,P). Occasionally senescent microglial cells, as defined by Streit (2006) could be identified with dystrophic processes, showing some extent of structural deterioration in aged animals, but these were rarely encountered (not shown).

Analysis of mRNA levels within hippocampal tissue revealed a significant age-related increase in GFAP mRNA (***$p < 0.001$; 2-way ANOVA; aged versus young vehicle-treated animals; Fig. 3A). S100ß mRNA also showed a modest age-related increase (***$p<0.001$; 2-way ANOVA; aged versus young; Fig. 3B). MHCII mRNA levels were previously shown to increase with age (*$p<0.05$; aged versus young vehicle-treated animals; Downer et al., 2009), mirroring the increase in MHCII immunoreactivity found in the present study.

Effects of FGL treatment on astrocyte and microglial cell responses in the hippocampus

Figures 4 and 5 highlight the effects of systemic treatment with FGL on astrocyte and microglial responses within the hippocampus in young (Fig. 4) and aged (Fig. 5) animals.

(i) FGL down-regulates GFAP immunoreactivity within the young and aged hippocampus

GFAP immunoreactivity was significantly reduced within the hippocampus and corpus callosum of young (4 month-old; Fig. 4A) and aged (22 month-old) animals treated with FGL (Fig. 5A; see also Fig. 1B',D',F',H',R'), with the exception of the CA1 subfield, which showed no significant change in older animals when examining group effects (Fig. 5A). Changes in the morphology of astrocytes were apparent: FGL-treated astrocytes adopted much thinner, and lengthened processes compared to their vehicle-treated counterparts (see for example Fig. 1D',F',H'). Analysis of GFAP mRNA levels within hippocampal tissue revealed a similar response to treatment with FGL, with a significant reduction in GFAP mRNA expression in aged animals (+$p<0.05$; 2-way ANOVA; aged vehicle-treated versus aged FGL-treated; Fig. 3A).

(ii) FGL has no effect on S100β+ cell density in young and aged animals

The immunostaining pattern for S100β, highlighting the prominent labelling of astrocyte cell bodies, is presented in Fig. 1I-P,J',L',N',P'). FGL treatment had no significant effect on S100ß+ cell density within any of the hippocampal areas examined in 4-month-old (Fig. 4B) and 22-month-old animals (Fig. 5B). Likewise, no clear qualitative change in cell numbers could be observed when visually inspecting sections (see for example, Fig. 1L,N,P and L',N',P'). FGL also failed to alter S100ß mRNA expression levels either in young or in aged animals (Fig. 3B). These observations were in stark contrast to the effect of FGL on microglia presented below.

(iii) FGL markedly reduces MHCII immunoreactivity within the aged hippocampus

CD11b and MHCII immunoreactivity were significantly reduced (by 2-7 fold) within the hippocampus and corpus callosum of 22 month old animals treated with FGL, both qualitatively (Fig. 2B',D',F',H',R' and Fig. 2J',L',N',P',T') and quantitatively (Fig. 5C,D). CD11b immunoreactivity was also reduced within the hippocampus of younger animals treated with

FGL (Fig. 4C), but the effects on MHCII immunoreactivity were not so clear at this age (although a small, opposite effect was noted within the DG/hilus; Fig. 4E).

(iv) FGL markedly reduces microglial cell density within the aged hippocampus

FGL treatment significantly lowered the mean MHCII+ cell density (around 2-fold) within the hippocampus of 22 month old animals (Fig. 5F). MHCII+ cell density values remained low, and were not significantly altered within the CA1 area (Fig.5F). Although mean cell density values for CD11b were reduced following FGL treatment in aged animals, these did not reach statistical significance (Fig. 5D). FGL treatment had no significant effect on mean CD11b+ and MHCII+ cell densities within the hippocampus of young animals (Fig. 4D,F).

Discussion

This study has investigated changes in microglial and astrocyte population densities, morphology, and phenotype within the hippocampus of aged compared with young rats, and assessed whether any age-related changes might be modulated by treatment with the NCAM-derived peptide, FGL. Using quantitative morphometric analyses, we have provided evidence *in situ* of widespread activation of glial cells within the dorsal hippocampus of aged rats, which is attenuated following treatment with FGL. These morphological data extend molecular and physiological observations concerning the neuroprotective and anti-inflammatory activities of FGL (Downer et al., 2010).

Age-related changes affecting astrocytes and microglia within the hippocampus

Our data indicate similar morphological responses in astrocytes and microglia within the dorsal hippocampus with age. Resident populations of astrocytes markedly upregulated GFAP and underwent morphological transformation to a more 'activated' state by 22 months (Fig.1 A-H). Microglia also underwent morphological transformation and this, together with the robust upregulation of CD11b in the CA1 and CA3 (Fig. 2,D,F,R) and MHC class II immunoreactivity within the CA3 and DG/hilus (see Fig. 2N,P,T), highlights an increase in the activation status of these cells in 22 month old rats. Like previous authors (Ogura et al., 1994; Rosovsky et al., 1998) we would consider the use of MHCII, as in our study, to represent a more appropriate discriminator of the microglial activation status, since this is differentially upregulated within the hippocampus with age (see Fig. 2). The comparatively low levels of MHCII immunoreactivity and minimal presence of MHCII+ cells within the CA1 area (Fig. 2K,L,S,T) is intriguing, particularly as this region is known to be selectively vulnerable in ageing and age-related diseases (Mueller et al., 2007). This novel observation and underlying mechanisms will

need to be explored in future studies (e.g. MHCII+ microglia could represent a subpopulation of resident cells, with distinct functional properties).

These results extend previous *in vivo* observations showing age-related activation of microglia (Htain et al., 1994; Lawson et al. 1990; Ogura et al., 1994) and astrocytes (Amenta et al., 1998; Bronson et al., 1993; David et al., 1997; Geinisman et al., 1978; Hughes and Lantos, 1987; Mandybur et al., 1989; Sturrock, 1980), accompanied by increased numbers of MHCII+ microglia within the brain (Ogura et al., 1994; Perry et al., 1993). GFAP protein and mRNA levels are also known to become elevated in aged rodent brains (see Fig. 3A; Goss et al. 1991; Kohama et al. 1995; O'Callaghan and Miller 1991; Nichols et al., 1993). Earlier studies noted similar age-related changes in morphological characteristics of astrocytes to those we have described (i.e. cells becoming more 'fibrous' in nature). Although astrocytes undergo age-related morphological transformation, former studies have found little or no age-related change in the density of these cells (Bjorklund et al., 1985; Geinisman et al., 1978; Landfield et al., 1977; Lindsey et al., 1979; Ling and Leblond 1973), including two more recent stereological studies (Bhatnagar et al., 1997; Long et al., 1998). With age therefore, the *primary* astrocytic change appears to be hypertrophy (an increase in fibrous character as shown by up-regulation of GFAP, reflecting an increase in the 'activation status' of astrocytes), rather than hyperplasia.

It is the basal, yet sustained, production of pro-inflammatory cytokines by activated neuroglial cells (e.g. higher expression of IL-1ß by aged microglia) that is thought to impact on brain ageing and cognitive processes. Microglial functions in particular are considered to change progressively from neuroprotective to neuroinflammatory and neurotoxic during ageing (Sawada et al., 2008; Sierra et al., 2007; von Bernhardi et al., 2010). Astrocytes and microglia derived from aged (24-month old) rat brains also demonstrate higher activation states in tissue culture, with microglia expressing higher levels of MHCII and astrocytes expressing higher levels of GFAP (Rozovsky et al., 1998). Microglia derived from healthy aged animals (i.e. *ex vivo*) display specific changes in their functional status, with increased mRNA expression of both pro-inflammatory (TNF-a, Il-1 ß, IL-6) and anti-inflammatory cytokines (IL-10, TGF-ß1) (Sierra et al., 2007). Such glial cell changes do not occur in isolation, but in the context of increased cellular stress responses (or deficiencies in cellular coping mechanisms), that are associated with ageing (Amenta et al., 1998; von Bernhardi et al., 2010). Collectively, glial cell activation in parallel with such physiological changes, has largely (although not exclusively, see for example Conde and Streit, 2006) been viewed as detrimental, contributing towards the cognitive decline seen in old age (von Bernhardi et al., 2010), and therefore a potential target for preventive treatment or 'prophylactic' therapy.

FGL attenuates age-related astrocyte activation but has no effect on astrocyte cell density in the hippocampus of aged animals

Systemic treatment with FGL effectively reduced the activation state of astrocytes (GFAP mRNA expression and immunoreactivity) within the dorsal hippocampus and corpus callosum of aged animals (with the exception of the CA1 subfield which showed no change at 22 months) (Fig. 5A). This effect could be mediated directly through binding of FGL to FGF receptors (primarily FGFR1 and FGFR2) on astrocytes, since the FGFR ligand FGF-2 (bFGF) has been shown to reduce GFAP mRNA and protein levels in astrocyte cultures maintained in vitro, and to inhibit the TGF-ß1-mediated increase in GFAP expression (Reilly et al., 1998). Astrocytes contain high levels of FGFR1 and FGFR2 mRNA (Gonzalez et al., 1995). Within the hippocampus, astrocytes are the primary source of FGFR1 and FGFR2 expression (Chadashvilli and Peterson, 2006). This suggests a role for the FGFR as a means for controlling progressive astrogliosis during ageing. However, the relationship of these findings to regional expression or functionality of FGFR on astrocytes within the hippocampus remains to be explored.

S100ß is a calcium-binding protein, known to be expressed by all types of astrocytes; it prominently labels astrocyte cell somata within the CNS (Rothermundt et al., 2003; Sen and Belli, 2007, Savchenko et al., 2002). We used S100ß labelling because it specifically identifies 'all populations' of astrocytes (including fibrous and protoplasmic, resident as well as activated), allowing us to reliably look at 'total' astrocyte population dynamics. We found that FGL treatment had no effect on S100ß+ cell density within the dorsal anterior hippocampus in either young (Fig. 4B) or aged (Fig. 5B) animals. This suggests that FGL has little impact on astrocytic proliferation, reported to be induced by FGF2 in a number of studies (Gomez-Pinilla et al., 1995; Chadashvili and Peterson, 2006; Jin et al., 2003; Yoshimura et al., 2001), and could indicate that FGL acts via a different intracellular signalling pathway to that activated by FGF2 in astrocytes. FGL treatment also failed to alter S100ß mRNA levels in aged animals (Fig. 3B).

FGL attenuates age-related microglial activation and significantly reduces microglial cell density in the hippocampus of aged animals

Systemic treatment with FGL markedly reduced microglial activation (as determined by CD11b and MHCII immunoreactivity) within the dorsal hippocampus and callosal white matter of aged animals (see Fig. 5C,E and Fig. 2R',T'). These findings were in agreement with a previous report which showed that treatment with FGL reduced MHCII mRNA levels within the hippocampus of 22 month-old rats (Downer et al., 2009). In the present study, the total volume of the dorsal hippocampus did not differ significantly in 22 month-old animals treated with

vehicle or FGL (p=0.807), so total hippocampal cell density measurements were not affected by volumetric changes between groups in these aged animals. We found that treatment with FGL significantly reduced MHCII+ (Fig. 5F) microglial cell density in aged animals. MHCII+ cell density was reduced by about 2 fold in the CA3 and DG/hilus (Fig. 5F). FGL therefore exerted a potent regulatory effect on the resident innate immune cells of the brain in ageing. Microglia, like astrocytes, have also been shown to express FGFRs (FGFR1-4; Liu et al., 1998; Presta et al., 1995), and upregulate FGFRs when activated (e.g. FGFR1; Liu et al., 1998). FGL could therefore exert its effects directly via FGFR1.

An alternative explanation is that FGL exerts its suppressive effects on glial cell activation indirectly. Apart from glial cells, FGFR expression can also be demonstrated widely on neurons, including within the hippocampus (e.g. FGFR1 and FGFR2; Gonzalez et al., 1995). There is evidence to indicate that FGL promotes neuronal expression of CD200 (Downer et al., 2009), known to be a key regulator of microglial activation within the nervous system (Biber et al., 2007). FGL also enhances release of IL-4 from glial cells (Downer et al., 2010) and this too may act as a downregulatory signal for microglial activation and may inhibit microglial proliferation (Kloss et al., 1997). However, since the route of administration of FGL was systemic, the fact that FGL might additionally be acting outside the nervous system to alter circulating levels of pro-and anti-inflammatory cytokines that may subsequently access the brain and influence glial cell responses, cannot be entirely excluded at present (see for example Godbout et al., 2005). Although it is clear that FGL attenuates microglial activation and reduces microglial density, the functional status of these cells, in particular their neuroinflammatory as opposed to neurotrophic and neuroprotective properties (Biber et al. 2007; Conde and Streit, 2006) will need to be examined further *in vivo*.

Our results provide convincing evidence to support a role for FGL in inhibiting age-related glial cell activation within the aged brain. FGL has been shown to restore cognitive function, enhance memory and avert neuropathology in models of ageing and age-related diseases (Downer et al., 2010; Cambon et al., 2004; Klementiev et al., 2007; Neiiendam et al., 2004; Popov et al., 2008; Skibo et al., 2005; Stewart et al., 2010). Together with its anti- inflammatory properties (Downer et al., 2009; Downer et al., 2010) our data highlight the potential for FGL to combat age-related changes in the brain, warranting further investigation into its therapeutic potential to alleviate age-related cognitive dysfunction. The evidence so far supports a potential therapeutic role for FGL in the *aged* brain. Given our observation that hippocampal volume estimates were reduced following treatment of young rats with FGL, the effect of FGL on the brain at younger stages still needs to be explored. The biological relevance of these volumetric differences is at present unclear, but could indicate specific effect(s) on developmental

trajectories that need to be taken into account when considering FGL treatment as a therapeutic strategy.

Acknowledgement

This study was supported by the European Union FPVI "Promemoria" programme grant (Contract No. 512012).

Disclosure Statement

The authors confirm that there are no conflicts of interest including any financial, personal or other relationships in relation to this work

References

Amenta, F., Bronzetti, E., Sabbatini, M., Vega, J.A., 1998. Astrocyte changes in aging cerebral cortex and hippocampus: a quantitative immunohistochemical study. Microsc Res Tech. 43, 29-33.

Anand, R., Seiberling, M., Kamtchoua, T., Pokorny, R., 2007. Tolerability, safety and pharmacokinetics of the FGL-L peptide, a novel mimetic of neural cell adhesion molecule, following intranasal administration in healthy volunteers. Clin. Pharmakokinet. 46, 351-358.

Barnes, C,A., 1988. Spatial learning and memory processes: the search for their neurobiological mechanisms in the rat. Trends Neurosci. 11, 163-169.

Berezin, V., Bock, E., 2004. NCAM mimetic peptides: pharmacological and therapeutic potential. J. Mol. Neurosci. 22, 33-39.

Berezin, V., Bock, E., 2010. NCAM mimetic peptides: an update. Adv Exp Med Biol. 663, 337-353.

Berezin, V., Bock, E., Poulsen, F., 2000. The neural cell adhesion molecule NCAM. Curr. Opin. Drug Disc. Devel. 3, 605-609.

Biber, K., Neumann, H., Inoue, K., Boddeke, HW., 2007. Neuronal „on. and „off. signals control microglia. Trends Neurosci. 30, 596-602.

Bjorklund, H., Eriksoddotter-Nilsson, M., Dahl, D., Rose, G., Hoffer, B., Olson, L., 1985. Image analysis of GFA-positive astrocytes from adolescence to senescence. Exp Brain Res. 58, 163-170.

Brey, E.M., Lalani, Z., Johnston, C., Wong, M., McIntire, L.V., Duke, P.J., Patrick, C.W.Jr. 2003. Automated selection of DAB-labeled tissue for immunohistochemical quantification. J. Histochem. Cytochem. 51, 575-584.

Bronson, R.T., Lipman, R.D., Harrison, D.E., 1993. Age-related gliosis in the white matter of mice. Brain. Res. 58, 124-128.

Bryan, R., Gekker, G., Hu, S., Sheng, W.S., Cheeran, M., Lokensgard, J.R., Peterson, P.K., 2004. Role of microglia in central nervous system Infections. Clin. Microbiol. Rev. 17, 942-964.

Cambon, K., Hansen, S.M., Venero, C., Herrero, AI., Skibo, G., Berezin, V., Bock, E., Sandi, C., 2004. A synthetic neural cell adhesion molecule mimetic peptide promotes synaptogenesis, enhances presynaptic function, and facilitates memory consolidation. J. Neurosci. 24, 4197-4204.

Campuzano, O., Castillo-Ruiz, M.M., Acarin, L., Castellano, B., Gonzalez, B. 2008. Distinct pattern of microglial response, cyclooxygenase-2, and inducible nitric oxide synthase expression in the aged rat brain after excitotoxic damage. J. Neurosci. Res. 86, 3170-3183.

Cavallaro, S., D.Agata. V., Manickam, P., Dufour, F., Alkon, DL., 2002. Memory-specific temporal profiles of gene expression in the hippocampus. Proc. Natl. Acad. Sci. USA. 99, 16279-16284.

Chadashvili, T., Peterson, DA., 2006. Cytoarchitecture of fibroblast growth factor receptor 2 (FGFR2) immunoreactivity in astrocytes of neurogenic and non-neurogenic regions of the young adult and aged rat brain. J. Comp. Neurol. 498, 1-15.

Clarke, R.M., Lyons, A., O.Connell, F., Deighan, B.F., Barry, C.E., Anyakoha, N.G., Nicolaou, A., Lynch, M.A., 2008. A pivotal role for IL-4 in atorvastatin-associated neuroprotection in rat brain. J. Biol. Chem. 283, 1808-1817.

Conde, J.R., Streit, W.J., 2006. Microglia in the aging brain. J. Neuropathol. Exp. Neurol. 65, 199203.

Cremer, H., Lange, R., Christoph, A., Plomann, M., Vopper, G., Roes, J., Brown, R., Baldwin, S., Kraemer, P., Scheff, S., Barthels, D., Rajewsky, K., Wille, W., 1994. Inactivation of the N-CAM gene in mice results in size reduction of the olfactory bulb and deficits in spatial learning. Nature. 367, 455-459.

Crossin, KL., Krushel, L.A., 2000. Cellular signaling by neural cell adhesion molecules of the immunoglobulin superfamily. Dev. Dyn. 218, 260-279.

David, J.P., Ghozali, F., Fallet-Bianco, C., Wattez, A., Delaine, S., Boniface, B., Di Menza, C., Delacourte, A., 1997. Glial reaction in the hippocampal formation is highly correlated with aging in human brain, Neurosci. Lett. 235, 53-56.

Dalmau, I., Vela, J. M., Gonzalez, B., Finsen, B., Castellano, B., 2003. Dynamics of microglia in the developing rat brain. J Comp Neurol 458, 144-57.

Dobson, L., Conway, C., Hanley, A., Johnson, A., Costello, S., O.Grady, A., Connolly, Y., Magee, H., O.Shea, D., Jeffers, M., Kay, E., 2010. Image analysis as an adjunct to manual HER-2 immunohistochemical review: a diagnostic tool to standardize interpretation. Histopathology 57, 27-38.

Downer, E.J., Cowley, T.R., Lyons, A., Mills, K.H.G., Berezin, V., Bock, E., Lynch, M.A., 2010. A novel anti-inflammatory role of NCAM-derived mimetic peptide, FGL. Neurobiol. Aging. 31, 118-128

Downer, E.J., Cowley, T.R., Cox, F., Maher, F.O., Berezin, V., Bock, E., Lynch, MA., 2009. A synthetic NCAM-derived mimetic peptide, FGL, exerts anti-inflammatory properties via IGF-1 and interferon-gamma modulation. J. Neurochem. 109, 1516-1525

Frautschy, S.A., Hu, W., Kim, P., Miller, S.A., Chu, T., Harris-White, M.E., Cole, G.M., 2001. Phenolic anti-inflammatory antioxidant reversal of Aß-induced cognitive deficits and neuropathology. Neurobiol. Aging. 22, 993-1005.

Geinisman, Y., Bondareff, W., Dodge, J.T., 1978. Hypertrophy of astroglial processes in the dentate gyrus of the senescent rat. Am. J. Anat. 153, 537-544.

Godbout, J.P., Chen, J., Abraham, J., Richwine, A.F., Berg, B.M., Kelley, K.W., Johnson, R.W., 2005. Exaggerated neuroinflammation and sickness behavior in aged mice following activation of the peripheral innate immune system. FASEB. J. 19, 1329-1331.

Gomez-Pinilla, F., Vu, L,, Cotman, C.W., 1995. Regulation of astrocyte proliferation by FGF-2 and heparan sulfate in vivo. J. Neurosci. 15, 2021-2029.

Gonzalez, A.M., Berry, M., Maher, P., Logan, A., Baird, A., 1995. A comprehensive analysis of the distribution of FGF-2 and FGFR1 in the rat brain. Brain. Res. 701, 201-226.

Goss, J.R., Finch, C.E., Morgan, D.G., 1991. Age-related changes in glial fibrillary acidic protein RNA in the mouse brain. Neurobiol. Aging. 12, 165-170.

Griffin, R., Nally, R., Nolan, Y., McCartney, Y., Linden, J., Lynch, M.A., 2006. The age-related attenuation in long-term potentiation is associated with microglial activation. J. Neurochem. 99, 1263-1272.

Hansen, S.M., Li, S., Bock, E., Berezin, V., 2010. Synthetic NCAM-derived ligands of the fibroblast growth factor receptor. Adv. Exp. Med. Biol. 663, 355-372

Himeda T, Watanabe., Y, Tounai, H., Hayakawa, N., Kato, H., Araki, T., 2006. Time-dependent alterations of co-localization of S100β and GFAP in the MPTP-treated mice. J Neural Transm. 113, 1887–1894

Htain, W.W., Leong, S.K., Ling, E.A., 1994. A comparative Mac-1 immunocytochemical and lectin histochemical study of microglia cells in normal and athymic mice. Glia. 12, 44-51.

Hughes, C.C.W., Lantos, P.L., 1987. A morphometric study of blood vessel, neuron and glial cell distribution in young and adult rat brain. J. Neurosci. 79, 101-110.

Jin, K., Sun, Y., Xie, L., Batteur, S., Mao, X.O., Smelick, C., Logvinova, A., Greenberg, D.A., 2003. Neurogenesis and aging: FGF-2 and HB-EGF restore neurogenesis in hippocampus and subventricular zone of aged mice. Aging. Cell. 2, 175-183.

Kiselyov, V.V., Skladchikova, G., Hinsby, A.M., Jensen, P.H., Kulahin, N., Soroka, V., Pedersen, N., Tsetlin, V., Poulsen, F.M., Berezin, V., Bock. E., 2003. Structural basis for a

direct interaction between FGFR1 and NCAM and evidence for a regulatory role of ATP. Structure. 11, 691-701.

Klementiev, B., Novikova, T., Novitskaya, V., Walmod, P.S., Dmytriyeva, O., Pakkenberg, B., Berezin, V., Bock, E., 2007. A neural cell adhesion molecule-derived peptide reduces neuropathological signs and cognitive impairment induced by Abeta25-35. Neuroscience. 145, 209-224.

Kloss, C.U., Kreutzberg, G.W., Raivich, G., 1997. Proliferation of ramified microglia on astrocyte monolayer: characterisation of stimulatory and inhibitory cytokines. J. Neurosci. Res. 49, 248-254.

Kohama. S.G., Goss, J.R., Finch, C.E., McNeill, T.H., 1995. Increases of glial fibrillary acidic protein in the aging female mouse brain. Neurobiol. Aging. 16, 59-97.

Kokolakis, G., Panagis, L., Stathopoulos, E., Giannikaki, E., Tosca, A., Krüger-Krasagakis, S., 2008. From the protein to the graph: how to quantify immunohistochemistry staining of the skin using digital imaging. J. Immunol. Meth. 331, 140-146.

Landfield, P.W., Rose, G., Sandles, L., Wohlstadter, T.C., Lynch, G., 1977. Patterns of astroglial hypertrophy and neuronal degeneration in the hippocampus of aged memory-deficient rats. J. Gerontol. 32, 3-12.

Lawson, L.J., Perry, V.H., Dri, P., Gordon, S., 1990. Heterogeneity in the distribution and morphology of microglia in the normal adult mouse brain. Neuroscience. 39, 151-170.

Leuba, G., Kraftsik, R., Saini, K., 1998. Quantitative distribution of parvalbumin, calretinin and calbindin D-28k immunoreactive neurons in the visual cortex of normal and Alzheimer cases. Exp. Neurol. 152, 278-291.

Lindsey, JD., Landfield, P., Lynch, G., 1979. Early onset and topographical distribution of hypertrophied astrocytes in hippocampus of aging rats: a quantitative study. J. Gerontol. 34, 661 671.

Ling, E.A., Leblond, C.P., 1973. Investigations of glial cells in semithin sections. II. Variation with age in the numbers of the various glial cell types in rat cortex and corpus callosum. J. Comp. Neurol. 149, 73-82.

Liu, X., Mashour, G.A., Webster, H.F., Kurtz, A., 1998. Basic FGF and FGF receptor 1 are expressed in microglia during experimental autoimmune encephalitis: temporally distinct expression of midkine and pleiotrophin. Glia. 24, 390-397.

Long, J.M., Kalehua, A.N., Muth, N.J., Calhoun, M.E., Jucker, M., Hengemihle, J.M., Ingram, D.K., Mouton, P.R., 1998. Stereological analysis of astrocyte and microglia in aging mouse hippocampus. Neurobiol. Aging. 19, 497-503.

Luthl, A., Laurent, J.P., Figurov, A., Muller, D., Schachner, M., 1994. Hippocampal long-term potentiation and neural cell adhesion molecules L1 and NCAM. Nature. 372, 777-779.

Lynch, A.M., Loane, D.J., Minogue, A.M., Clarke, R.M., Kilroy, D., Nally, R.E., Roche, O.J., O.Connell, F., Lynch, MA., 2007. Eicosapentaenoic acid confers neuroprotection in the amyloid-beta challenged aged hippocampus. Neurobiol. Aging. 28, 845-855.

Lynch, A.M., Lynch, M.A., 2002. The age-related increase in IL-1 type I receptor in rat hippocampus is coupled with an increase in caspase-3 activation. Eur. J. Neurosci. 15, 1779-1788.

Lynch, M.A., 2004. Long-term potentiation and memory. Physiol. Rev. 84, 87-136.

Mandybur, T.I., Ormsby, I., Zelman, FP., 1989. Cerebral aging: a quantitative study of gliosis in old nude mice. Acta. Neuropathol. 7, 507-513.

Milnerwood, A.J., Cummings, D.M., Dallerac, G.M., Brown, J.Y., Vatsavayai, S.C., Hirst, M.C., Rezaie, P., Murphy, K.P.S.J., 2006. Early development of aberrant synaptic plasticity in a mouse model of Huntington.s disease. Hum. Mol. Genet. 15, 1690-1703.

Mueller, S.G., Stables, L., Du, A.T., Schuff, N., Truran, D., Cashdollar, N., Weiner, M.W., 2007. Measurement of hippocampal subfields and age-related changes with high resolution MRI at 4 T. Neurobiol. Aging. 28, 719-726.

Murray, C.A., Lynch, M.A., 1998. Evidence that increased hippocampal expression of the cytokine interleukin-1 beta is a common trigger for age and stress-induced impairments in long-term potentiation. J. Neurosci. 18, 2974-2981.

Neiiendam, J.L., Kohler, L.B., Christensen, C., Li, S., Pedersen, M.V., Ditlevsen, D.K., Kornum, M.K., Kiselyov, V.V.,Berezin, V., Bock, E., 2004. An NCAM-derived FGF-receptor agonist, the FGL-peptide, induces neurite outgrowth and neuronal survival in primary rat neurons. J. Neurochem. 91, 920-935.

Nichols, N.R., Day, J.R., Laping, N.J., Johnson, S.A., Finch, C.E., 1993. GFAP mRNA increases with age in rat and human brain. Neurobiol. Aging. 14, 421-429.

O'Callaghan, J.P., Miller, D.B., 1991. The concentration of glial fibrillary acidic protein increases with age in the mouse and rat brain. Neurobiol. Aging. 12, 171-174.

Ogura, K., Ogawa, M., Yoshida, M., 1994. Effects of aging on microglia in the normal rat brain: immunohistochemical observations. Neuroreport. 5, 1224-1226.

Pakkenberg, B., Gundersen, H.J., 1997. Neocortical neuron number in humans: effect of sex and age. J. Comp. Neurol. 384, 312-320.

Paxinos, G., Watson, C., 2007. The rat brain in stereotactic co-ordinates. Academic Press, 6th edition

Pelinka, L.E., Kroepfl, A., Leixnering, M., Buchinger, W., Raabe, A., Redl, H., 2004. GFAP versus S100B in serum after traumatic brain injury: relationship to brain damage and outcome. J Neurotrauma. 11, 1553-1561.

Peretti-Renucci, R., Feuerstein, C., manier, M., Lorimier, P., Savasta, M., Thibault, J., Mons, N., Geffard, M., 1991. Quantitative image analysis with densitmetry for

immunohistochemistry and autoradiography of receptor binding sites – methodological considerations. J. Neurosci. Res. 28, 583-600.

Perry, V.H., Matyszak, M.K., Fearn, S., 1993. Altered antigen expression of microglia in the aged rodent CNS. Glia. 7, 60-67.

Pontikis, C.C., Cella, C.V., Parihar, N., Lim, M.J., Chakrabarti, S., Mitchison, H.M., Mobley, W.C., Rezaie. P., Pearce, D.A., Cooper, J.D., 2004. Late onset neurodegeneration in the Cln3-/-mouse model of juvenile neuronal ceroid lipofuscinosis is preceded by low level glial activation. Brain. Res. 1023, 231-242.

Popov, V.I., Davies, H.A., Rogachevskii, V.V., Errington, M.L., Gabbott, P.L.A., Bliss, T.V.P., Stewart, M.G., 2004. Remodelling of synaptic morphology but unchanged synaptic density during late phase LTP: a serial section EM study of the dentate gyrus in the anaesthetised rat. Neuroscience 28, 251-262.

Popov, V.I., Medvedev, N.I., Kraev I.V., Gabbott, P.L., Davies, H.A., Lynch, M., Cowley, T.R., Berezin, V., Bock, E., Stewart, M.G., 2008. A cell adhesion molecule mimetic, FGL peptide, induces alterations in synapse and dendritic spine structure in the dentate gyrus of aged rats: a three-dimensional ultrastructural study. Eur. J. Neurosci. 27, 301-314.

Presta, M., Urbinati, C., Dell.era, P., Lauro, G.M., Sogos, V., Balaci, L., Ennas, M.G., Gremo, F., 1995. Expression of basic fibroblast growth factor and its receptors in human fetal microglia cells. Int. J. Dev. Neurosci. 13, 29-39.

Reilly, J.F., Maher, P.A., Kumari, V.G., 1998. Regulation of astrocyte GFAP expression by TGF- and FGF-2. Glia. 22, 202–210.

Rezaie, P., Pontikis, C.C., Hudson, L., Cairns, N.J., Lantos, P.L., 2005. Expression of cellular prion protein in the frontal and occipital lobe in Alzheimer.s disease, diffuse Lewy body disease, and in normal brain: an immunohistochemical study. J. Histochem. Cytochem. 53, 929-940. neurodegeneration. Miscrosc. Res. Tech. 60, 614-632.

Rozovsky, I., Finch, C.E., Morgan, T.E., 1998. Age-related activation of microglia and astrocytes: in vitro studies show persistent phenotypes of aging, increased proliferation, and resistance to down-regulation. Neurobiol. Aging. 19, 97-103.

Savchenko, V.L., Mckanna, J.A., Nikonenko, I.R., Skibo, G.G., 2000. Microglia and astrocytes in the adult rat brain: comparative immunocytochemical analysis demonstrates the efficacy of lipocortin 1 immunoreactivity. Neuroscience. 96, 195-203.

Sawada, M., Sawada, H., Nagatsu, T., 2008. Effects of aging on neuroprotective and neurotoxic properties of microglia in neurodegenerative diseases. Neurodegener. Dis. 5, 254-256.

Secher, T., Berezin, V., Bock, E., Glenthøj, B., 2008. Effect of an NCAM mimetic peptide FGL on impairment in spatial learning and memory after neonatal phencyclidine treatment in rats. Behav Brain. Res. 199, 288-297.

Secher, T., Novitskaia, V., Berezin, V., Bock, E., Glenthoj, B., Klementiev, B., 2006. A neural cell adhesion molecule-derived fibroblast growth factor receptor agonist, the FGL-peptide, promotes early postnatal sensorimotor development and enhances social memory retention. Neuroscience. 141, 1289-1299.

Sen, J.G., Belli, A., 2007. S100beta in neuropathologic states: the CRP of the brain? J. Neurosci. Res. 85, 1373-1380.

Sheng, J.G., Mrak, R.E., Griffin, W.S., 1998. Enlarged and phagocytic, but not primed, interleukin 1aimmunoreactive microglia increase with age in normal human brain. Acta. Neuropathol. 95, 229-234.

Sierra. A., Gottfried-Blackmore, A.C., McEwen, B.S., Bulloch, K., 2007. Microglia derived from aging mice exhibit an altered inflammatory profile. Glia. 55, 412-424.

Skibo, G.G., Lushnikova, I.V., Voronin, K.Y., Dmitrieva, O., Novikova, T., Klementiev, B., Vaudano, E., Berezin, V.A., Bock, E., 2005. A synthetic NCAM-derived peptide, FGL, protects hippocampal neurons from ischemic insult both in vitro and in vivo. Eur. J. Neurosci. 22,15891596.

Stewart, M.G., Davies, H.A., Sandi, C., Kraev, I.V., Rogachevsky, V.V., Rodriguez, J.J., Cordero, I.M., Donohue, H.S., Gabbott, P.L.A., Peddie, C.J., Popov, V.I., 2005. Stress suppresses and learning induces expression of ultrastructural plasticity in CA3 of rat hippocampus: a 3dimensional ultrastructural study of thorny excrescences and their post synaptic densities. Neuroscience. 131, 43-54.

Stewart, M., Popov, V., Medvedev, N., Gabbott, P., Corbett, N., Kraev, I., Davies, H., 2010. Dendritic spine and synapse morphological alterations induced by a neural cell adhesion molecule (NCAM) mimetic. Adv. Exp. Med. Biol. 663, 373-383.

Streit, W.J., 2006. Microglial senescence: does the brain.s immune system have an expiration date? Trends Neurosci. 29, 506-510.

Sturrock, R.R., 1980. A comparative quantitative and morphological study of aging in the mouse neostriatum, indusium griseum and anterior commissure. Neuropathol. Appl. Neurobiol. 6, 51-68.

Von Bernhardi, R., Tichauer, J.E., Eugenin, J., 2010. Aging-dependent changes of microglial cells and their relevance for neurodegenerative disorders. J. Neurochem. 112, 1099-1114.

Walmod, P.S., Kolkova, K., Berezin, V., Bock, E., 2004. Zippers make signals: NCAM mediated molecular interactions and signal transduction. Neurochem. Res. 29, 2015-35.

Wang, C.J., Zhou, Z.G., Holmqvist, A., Zhang, H., Li, Y., Adell, G., Sun, X.F., 2009. Survivin expression quantified by Image Pro-Plus compared with visual assessment. Appl. Immunohistochem. Mol. Morphol. 17, 530-535.

Xavier, L.L., Viola, G.G., Ferraz, A.C., Da Cunha, C., Deonizio, J.M.D., Netto, C.A., Achaval, M., 2005. A simple and fast densitometric method for the analysis of tyrosine hydroxylase

immunoreactivity in the substantia nigra pars compacta and in the ventral tegmental area. Brain Res. Prot. 16, 58-64.

Yasuda, Y., Tateishi, N., Shimoda, T., Satoh, S., Ogitani, E., Fujita, S., 2004. Relationship between S100beta and GFAP expression in astrocytes during infarction and glial scar formation after mild transient ischemia. Brain Res. 1021, 20-31.

Yoshimura, S., Takagi, Y., Harada, J., Teramoto, T., Thomas, S.S., Waeber. C., Bakowska, J.C., Breakefield, X.O., Moskowitz, M.A., 2001. FGF-2 regulation of neurogenesis in adult hippocampus after brain injury. PNAS. 98, 5874-5879.

Zehntner, S.P., Chakravarty, M.M., Bolovan, R.J., Chan, C., Bedell, B.J., 2008. Synergistic tissue counterstaining and image segmentation techniques for accurate, quantitative immunohistochemistry. J. Histochem. Cytochem. 56, 873-880.

Figure 1. FGL treatment modulates astrocyte activation (morphology and phenotype) in the aged hippocampus

Micrographs showing GFAP and S100β (astrocyte) immunoreactivity, detected using a standardized immunohistochemical protocol, within the corpus callosum (CC) and hippocampus of young (4 month-old) and aged (22 month-old) rats treated with vehicle (A-H, I-P, Q-T), and following treatment with FGL in an aged animal (B',D',F',H',R' and J',L',N',P',T'). High power micrographs (A-H) and lower power micrographs (Q,R) demonstrate clearly that GFAP immunoreactivity is upregulated in older (B,D,F,H,R) compared to younger (A,C,E,G,Q) animals within all subfields examined. Age-related changes in the morphologies of astrocytes can also be observed, with GFAP+ astrocytes displaying thicker, and more stout processes. S100β immunoreactivity showed little appreciable change in older (J,L,N,P,T) compared to younger (I,K,M,O,S) animals. Treatment with FGL lowered GFAP immunostaining within the hippocampus and corpus callosum at 22 months. The response was particularly evident in the corpus callosum (B,B'), CA3 (F,F'), and DG (H,H'). S100ß immunostaining was not noticeably affected by treatment with FGL at 22 months (J',L',N',P',T'). The scale bar in (T') represents 65µm in A-P' and 733µm in Q-T'. Abbreviations: CC (corpus callosum), CA1 (hippocampal CA1 area), CA3 (hippocampal CA3 area), DG (dentate gyrus/hilus of the hippocampus).

Figure 2. FGL treatment modulates microglial activation (morphology and phenotype) in the aged hippocampus

Micrographs showing CD11b and MHCII (microglial) immunoreactivity, detected using a standardized immunohistochemical protocol, within the corpus callosum (CC) and hippocampus of young (4 month-old) and aged (22 month-old) rats treated with vehicle (A-H, I-P, Q-T), and following treatment with FGL in an aged animal (B',D',F',H',R' and J',L',N',P',T'). High power micrographs (A-H and I-P) and lower power micrographs (Q,R and S,T) demonstrate that CD11b and MHCII immunoreactivity is upregulated in older (R,T) compared to younger (Q,S) animals within the hippocampus. Age-related changes in the morphologies of microglia can also be observed, with MHCII+ and CD11b+ microglia adopting a bushy appearance (the former phenotype only rarely encountered within the CA1 area: K,L). Note also the differential phenotypic response of microglia with age, particularly in the CA1 and the DG/hilus (compare C,D with K,L and G,H with O,P). Lower power photographs (Q-T) show coronal sections taken through the dorsal hippocampus of 22 month old rats, immunostained for CD11b (Q,R) and MHCII (S,T). Note the widespread distribution of CD11b+ microglia (R) compared to the selective distribution of MHCII+ microglia within the CA3, DG/hilus and corpus callosum (T) at 22 months. Treatment with FGL dramatically lowered MHCII (L',N',P',T') and CD11b immunostaining (D',F',H',R') within the hippocampus at 22 months of age. The scale bar in (T') represents 65µm in A-P' and 733µm in Q-T'. Abbreviations: CC (corpus callosum), CA1 (hippocampal CA1 area), CA3 (hippocampal CA3 area), DG (dentate gyrus/hilus of the hippocampus).

Figure 3. FGL exerts differential effects on GFAP and S100β mRNA expression levels in the aged hippocampus

Analysis of mRNA expression levels, isolated from hippocampal tissue at 4 and 22 months of age, revealed a significant (nearly 3-fold) increase in GFAP mRNA levels with age (A) (***$p<0.001$; 2-way ANOVA), and a relatively mild increase in S100ß mRNA expression (B) (***$p<0.001$; 2-way ANOVA). FGL treatment partially reversed the age-related increase in GFAP mRNA (+ $p<0.05$ aged vehicle-treated versus aged FGL-treated) (A), but had no significant effect on S100ß mRNA expression (B).

Figure 4. Effect of FGL treatment on astrocyte and microglial responses (phenotype and population densities) within the hippocampus of young rats

Quantitative analysis of GFAP, CD11b and MHCII immunoreactivity within the corpus callosum and hippocampus of rats treated with vehicle or FGL at 4 months of age is shown in (A,C,E). The graphs show mean percentage immunoreactivity (% Area) per microscopic field, determined by optical segmentation (as outlined in the Materials and Methods). FGL treatment significantly reduced GFAP immunoreactivity within the hippocampus in 4 month-old animals (A). CD11b immunoreactivity was also significantly lowered within the hippocampus (C), but there was no appreciable effect on MHCII immunoreactivity in the CC, CA1, or CA3 (although the DG/hilus showed a slight increase) at this age (E). The effect of FGL treatment on S100β+, CD11b+ and MHCII+ cell density (number of cells/mm^2) is shown in (B,D,F). Treatment with FGL did not alter S100β cell density (B), and had no *statistically significant* effect on either CD11b+ (D) or MHCII+ (F) cell densities within the hippocampus at 4 months of age. Abbreviations: CC (corpus callosum), CA1 (hippocampal CA1 area), CA3 (hippocampal CA3 area), DG (dentate gyrus/hilus of the hippocampus), Total (mean total hippocampal value). Data are plotted as mean values ± SEM (n=5 animals per group). A minimum of 30 individual microscopic fields were analysed per region, per animal (see Materials and Methods). Asterisks denote statistical significance as follows: (*) $p<0.05$, (**) $p<0.01$, (***) $p<0.001$. NS: not significant.

Figure 5. FGL modulates astrocyte and microglial responses (phenotype and cell density) within the aged rat hippocampus

Quantitative analysis of GFAP, CD11b and MHCII immunoreactivity within the corpus callosum and hippocampus of rats treated with vehicle or FGL at 22 months of age is shown in (A,C,E). The graphs show mean percentage immunoreactivity (% Area) per microscopic field, determined by optical segmentation (as outlined in the Materials and Methods). FGL treatment significantly reduced GFAP immunoreactivity within the hippocampus in 22 month-old animals (with the notable exception of the CA1 area) (A). CD11b immunreactivity was also significantly lowered within the corpus callosum and hippocampus (C). MHCII immunoreactivity was significantly lowered within the corpus callosum, CA3 and DG (by 2-7 fold) following FGL treatment at 22 months, but minimal within the CA1 area in both treated and vehicle groups (E). The effect of FGL treatment on S100ß+, CD11b+ and MHCII+ cell density (number of cells/mm^2) is shown in (B,D,F). Treatment with FGL did not alter S100β+ cell density (B), and had no *statistically significant* effect on CD11b+ cell density (D), but did specifically reduce the mean MHCII+ cell density (up to 2-fold) within the CA3 and DG/hilus (F) in aged animals. Abbreviations: CC (corpus callosum), CA1 (hippocampal CA1 area), CA3 (hippocampal CA3 area), DG (dentate gyrus/hilus of the hippocampus), Total (mean total hippocampal value). Data are plotted as mean values ± SEM (n=5 animals per group). A minimum of 30 individual microscopic fields were analysed per region, per animal (see Materials and Methods). Asterisks denote statistical significance as follows: (*) $p<0.05$, (**) $p<0.01$, (***) $p<0.001$. NS: not significant.

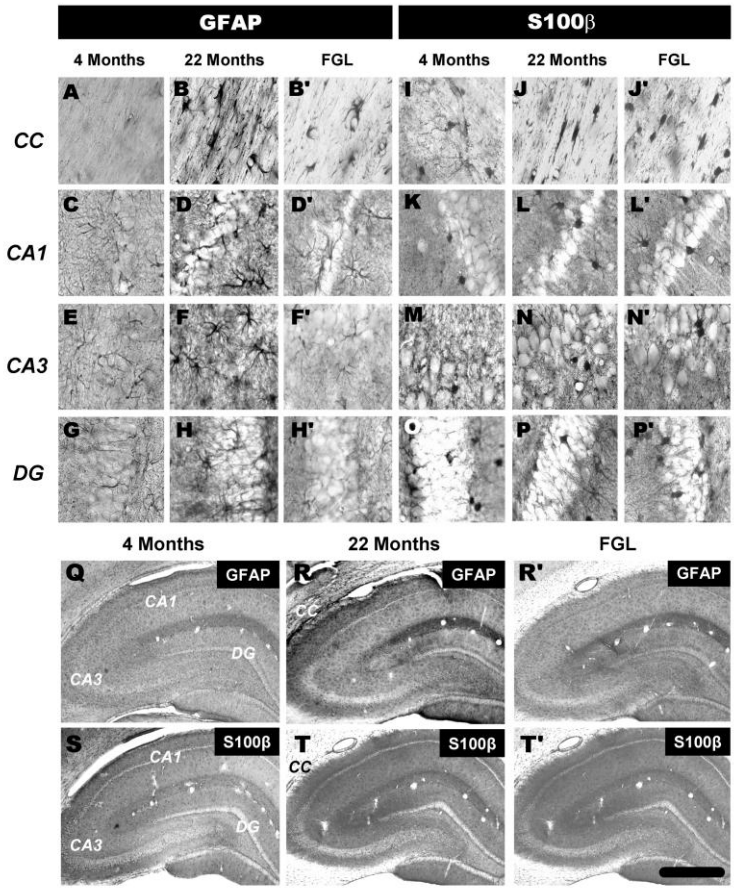

Fig 1

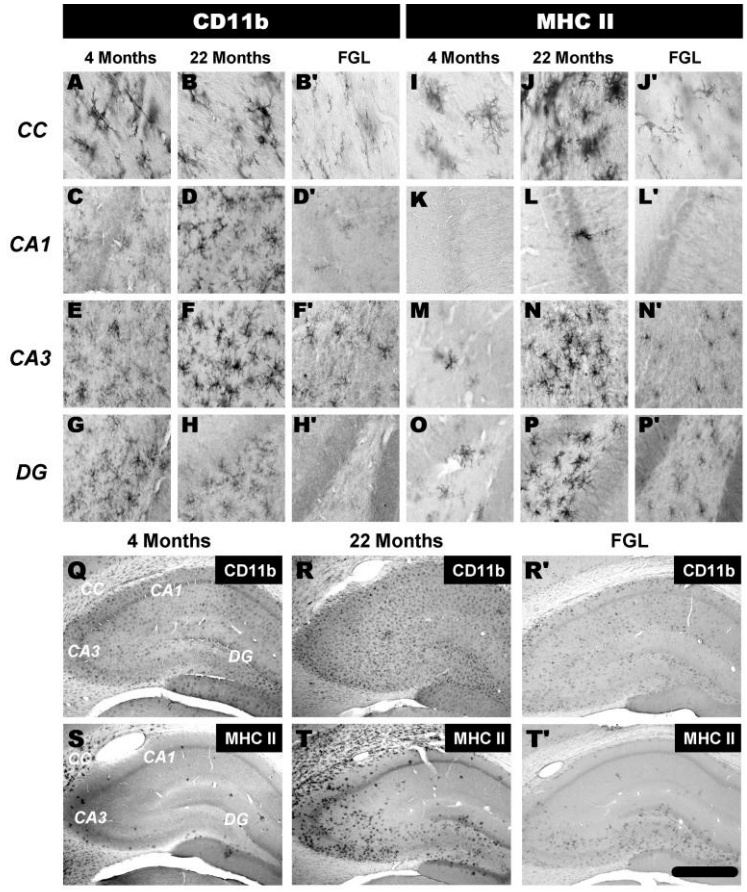

Fig 2

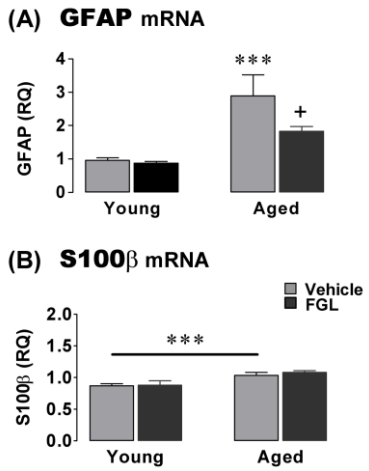

Fig 3

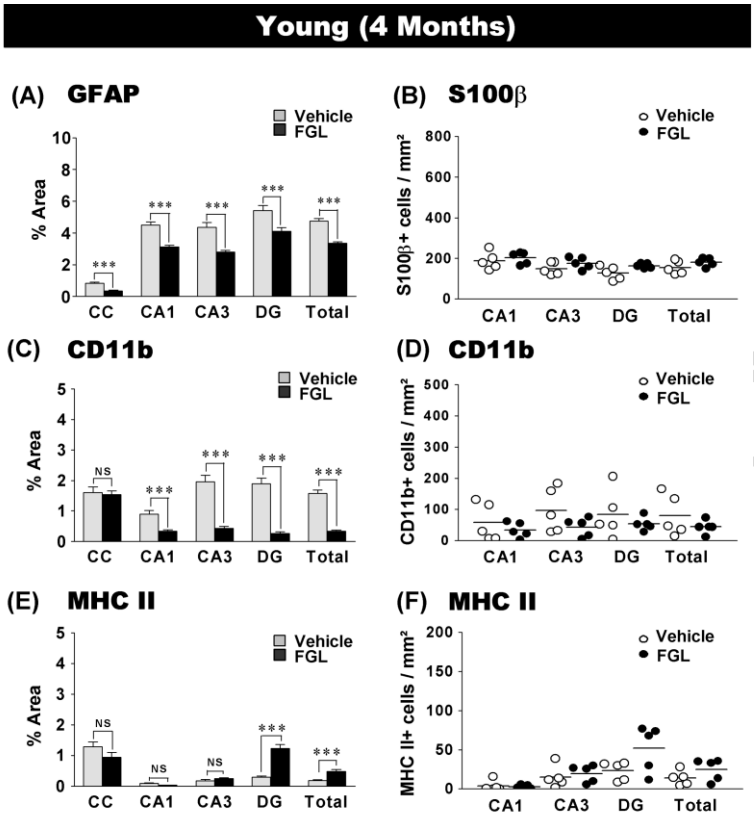

Fig 4

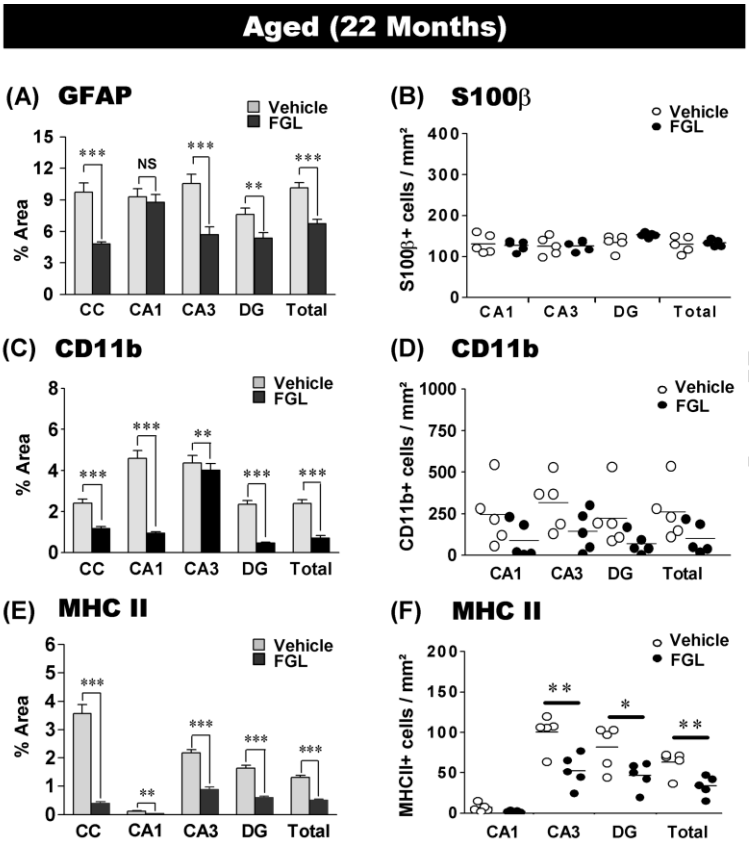

Fig 5

Ojo et al Highlights

- Quantitative morphometric methods and image analyses have shown the remarkable ability of a neural cell adhesion molecule mimetic (FGL) administered subcutaneously to attenuate a major feature of ageing, glial cell activation
- FGL treatment significantly reduced the density of CD11b+ and MHCII+ microglia in aged animals, concomitant with a reduction in immunoreactivity for these phenotypic markers